

Structural characterization of intrinsically curved AT-rich DNA sequences

Pilar Carrera and Fernando Azorín*

Departament de Biologia Molecular i Cellular, Centre d'Investigació i Desenvolupament-CSIC, Jordi Girona Salgado 18-26, 08034 Barcelona, Spain

Received June 30, 1994; Revised and Accepted August 10, 1994

ABSTRACT

AT-rich DNA sequences other than A_nT_m tracts ($n+m \geq 4$) are known to be intrinsically curved. The AATAT-element constitutes one known example of these sequences. In this paper, the elucidation of the structural basis of the curvature induced by this sequence element was addressed. As judged by the patterns of cleavage by the hydroxyl radical and DNase I, the AATAT sequence shows a narrow minor groove. Furthermore, the 5' adenine residue of the AA dinucleotide contained within the sequence is hyperreactive to diethylpyrocarbonate. Similar structural properties are shown by several sequences inducing intrinsic DNA curvature, such as an A_5 -tract or the closely related ATAAT, AATATA and TAATAT sequences, which are also shown here to induce curvature. On the other hand, other related sequences, such as TATAA and ATATA, that do not induce curvature, show different structural characteristics.

INTRODUCTION

Intrinsic curvature is a sequence dependent property of the DNA molecule. Intrinsically curved DNA is nearly ubiquitous and elements of curved DNA have been found to occur in many DNA molecules. Intrinsic DNA curvature is generally associated with the presence of A_nT_m tracts ($n+m \geq 4$), periodically spaced along the DNA molecule with a period close to the helical repeat (see 1–3 for reviews). More recently, DNA sequences containing other combinations of adenine and thymine residues were also shown to be curved (4–6). In particular, the sequence element AATAT was determined to be curved, contributing significantly to the intrinsic curvature of the mouse satellite DNA repeat (6). Finally, some GC-rich DNA sequences have also been found curved (4, 5, 7, 8).

Essentially two types of models were proposed to account for intrinsic DNA curvature. In a first group of models, curvature arises from the differential structural conformation of the sequence elements inducing the curvature (9–12). In these models deflection of the helical axis occurs principally at the junction between the structurally altered curving elements and the surrounding B-type DNA, and is manifested by changes in

either tilt or roll. In the second group of models, DNA curvature is the consequence of the vectorial addition of the deflections of the helical axis occurring at each individual dinucleotide step (1, 4, 5, 13–16). A particular wedge angle, which has components of tilt and roll, is associated with each type of dinucleotide step. Depending on the precise nucleotidic sequence, this vectorial sum may or may not result in a net deviation of the helical axis.

In this paper, the structural characteristics of the AATAT sequence element were investigated through the determination of its patterns of reactivity with the hydroxyl radical ($\cdot\text{OH}$), diethylpyrocarbonate (DEPC) and DNase I. Our results indicate that this sequence element shows an altered structural conformation which is manifested by a narrowing of the minor groove and a distorted conformation of the AA dinucleotide. The extent to which these structural properties determine the curvature induced by this sequence element was also investigated.

MATERIALS AND METHODS

DNAs

Oligonucleotides were synthesized in an Applied Biosystems automatic synthesizer and they were purified by polyacrylamide gel electrophoresis. For cloning into pUC19, oligonucleotides were self-ligated with T4 DNA ligase and the ligated products were cloned into the unique *Sma*I site of pUC19 after treatment with the Klenow enzyme. Cloned oligonucleotides were sequenced according to (17).

Polyacrylamide gel electrophoresis analysis

The electrophoretic analysis of the different oligonucleotides studied here was performed as described before (6). Briefly, synthetic oligonucleotides were annealed, 5'-end labelled with [γ - ^{32}P]ATP and T4 polynucleotide kinase, self-ligated and resolved in non denaturing 8% polyacrylamide gels run in 44.5 mM Tris–borate, 1.25 mM EDTA, pH 8.3. Electrophoresis were performed in a water-jacketed apparatus at either 4°C or 40°C. After electrophoresis gels were dried and autoradiographs were recorded on Hyperfilm (Amersham). For quantitative analysis of the results, autoradiographs were scanned with a MolecularDynamics laser densitometer. Oligomers of the 18-mer of sequence $d(\text{TTAGGG}\cdot\text{AACCCCT})_3$ were used as molecular

*To whom correspondence should be addressed

weight standards and the apparent molecular weights, in base pairs, were determined from the corresponding regression curves. The R_L values are expressed as apparent length/ actual length.

Hydroxyl radical cleavage

Cloned oligonucleotides were liberated from pUC19 by cleavage with *EcoRI*+*HindIII* which produces DNA fragments carrying several repeats of the corresponding synthetic oligonucleotide. These fragments were labelled at either the *EcoRI* or the *HindIII* site with [α - 32 P]dATP and the Klenow enzyme before cleavage with the second restriction endonuclease. The labelled fragments were purified by gel electrophoresis and then subjected to the reaction with the hydroxyl radical (\cdot OH) essentially as described before (6). About 50 ng of purified fragment were subjected to \cdot OH cleavage for 90 sec at 4°C in the presence of 500 ng of *E. coli* DNA in 10 mM Tris, 20 mM NaCl, pH 7.4. When cleavage was performed at 20°C, the reaction was allowed to proceed for 30 sec. Reactions were stopped by the addition of 20 μ l of 0.1 M thiourea. DNAs were then precipitated with ethanol and analysed on 8% polyacrylamide-7 M urea denaturing gels. Autoradiographs were recorded in Hyperfilm (Amersham) and scans obtained in a MolecularDynamics laser densitometer.

DNase I digestion

For DNase I digestion, labelled fragments carrying several copies of the corresponding synthetic oligonucleotide were obtained as described above and then subjected to DNase I (Boehringer) digestion at 4°C in a final volume of 8 μ l at different enzyme/DNA ratios for 1 min in the presence of 500 ng of calf thymus DNA in a buffer containing 20 mM MgCl₂, 20 mM NaCl, 4 mM MnCl₂, 10 mM Tris-HCl, pH 7.4. The reaction was stopped by the addition of 2 μ l of 80% formamide, 20 mM EDTA, pH 8. Cleavage products were resolved on denaturing polyacrylamide gels and autoradiographs recorded as described before. For quantitative analysis of the results, scans were obtained in a MolecularDynamics laser densitometer. The intensity of each band (I) was determined as the area underneath the corresponding peak on the densitometer scan and normalized with respect to the sum of the intensities of all bands (I_t). The relative frequency of cleavage at each phosphodiester bond was then expressed as the $\ln(I/I_t)$. The three-bond running average of cleavage was obtained by averaging the frequency of cleavage of each individual step with those of its nearest neighbours.

DEPC modification

For DEPC modification fragments were obtained as described before and then subjected to reaction with 2 μ l of DEPC (Fluka) at 4°C for 90 min in a final volume of 25 μ l in the presence of 100 ng of calf thymus DNA in a buffer containing 10 mM Tris-HCl, 20 mM NaCl, pH 7.4. The reaction was stopped by ethanol precipitation. Modified fragments were then subjected to cleavage with 1M piperidine at 90°C for 30 min and the cleavage products analysed on denaturing polyacrylamide gels as described before.

RESULTS

Curvature induced by the AATAT sequence depends strongly on its precise nucleotidic sequence

To study the influence of the nucleotidic sequence on the degree of curvature induced by the AATAT sequence element, we analyze the electrophoretic behaviour of oligonucleotides in which the position of the AA dinucleotide within the sequence was permuted (Table I). Oligo(AATAT), in which the AA dinucleotide occupies the further most 5' position on the AT-rich sequence, shows the highest electrophoretic retardation. At 4°C, the R_L value of 160 bp long oligomers of this oligonucleotide is 1.47 which, as expected for a curved DNA molecule, decreases strongly as temperature is increased to 40°C. Similar results were obtained earlier (6). On the other hand, oligo(TAATA) and oligo(TATAA), in which the ApA dinucleotide was moved in the 3' direction one or three steps respectively, do not appear to be significantly curved. They show, at 4°C, R_L values close to one which decrease only slightly when the electrophoresis is carried out at 40°C. Furthermore, a very similar R_L value is observed in the case of oligo(ATATA), which contains an alternating AT sequence which is known not to induce any intrinsic curvature. An intermediate situation is found in the case of oligo(ATAAT). In this case the R_L value at 4°C is 1.31, lower than that corresponding to oligo(AATAT), but significantly higher than those corresponding to oligo(TAATA) and oligo(TATAA). The degree of the curvature induced by the ATAAT sequence appears to be significantly lower than that induced by the AATAT-element as reflected by its smaller R_L value. In agreement with this interpretation, oligo(ATAAT) does not show any significant retardation when the electrophoresis is carried out at 20°C, while

Table I. R_L Values of the oligonucleotides used in these experiments

Oligonucleotide	Sequence	4°C	R_L	40°C
oligo(AATAT)	(tgg AATAT gatgg AATAT ga) _n	1.47 (±0.06)		1.09 (±0.01)
oligo(TAATA)	(tgg TAATA gatgg TAATA ga) _n	1.13 (±0.02)		1.03 (±0.03)
oligo(ATAAT)	(tgg ATAAT gatgg ATAAT ga) _n	1.31 (±0.01)		1.02 (±0.02)
oligo(TATAA)	(tgg TATAA gatgg TATAA ga) _n	1.12 (±0.01)		1.04 (±0.02)
oligo(ATATA)	(tgg ATATA gatgg ATATA ga) _n	1.12 (±0.01)		1.04 (±0.02)
oligo(A ₅ -AATAT)	(tgg AATAT gacAAAAAcggc) _n	1.74 ¹ (±0.06)		1.17 ¹ (±0.02)
oligo(AATATA)	(tgg AATATA gatgg AATATA g) _n	1.50 (±0.02)		1.14 (±0.02)
oligo(TAATAT)	(tgg TAATAT gtgg TAATAT g) _n	1.42 (±0.01)		1.08 (±0.03)
oligo(TTAGGG) ²	(ttagggttagggttaggg) _n	1.00		1.00

The R_L values (apparent length/actual length), at 4°C and 40°C, corresponding to 160 bp long oligomers of the indicated oligonucleotides are shown. Numbers in within parenthesis correspond to the error bars. The AT-region of each oligonucleotide is shown in bold-face.

¹ R_L values corresponding to oligo(A₅-AATAT) are taken from reference 6.

²Oligo(TTAGGG) corresponds to the 18-mer used as molecular weight standard.

oligo(AATAT) still shows some retardation at this temperature (not shown). At 40°C, the R_L value of oligo(ATAAT) is also close to one.

Oligonucleotides detected as intrinsically curved by polyacrylamide gel electrophoresis, but not those showing R_L values close to 1, show a sinusoidal pattern of hydroxyl radical (\cdot OH) cleavage

Intrinsically curved DNA molecules are known to have a differential sensitivity to the hydroxyl radical (\cdot OH), showing a characteristic sinusoidal pattern of \cdot OH cleavage (6, 18–20). In general, the waves of \cdot OH reactivity are phased with respect to the sequence elements introducing the curvature, the frequency of cleavage decreasing in the 5' to 3' direction. Instead, straight B-DNA is cleaved by \cdot OH nearly equally at each base step (21). Figure 1, shows the patterns of \cdot OH cleavage corresponding to the oligonucleotides described in Table I. Oligo(AATAT) shows a pattern of cleavage which is clearly sinusoidal (Figure 1B). The maxima of cleavage occur three or four bases upstream from the AT-rich sequence. Minimum frequency of cleavage is always observed at the thymine residue located immediately 3' from the AA dinucleotide. A very similar pattern of \cdot OH cleavage of the AATAT sequence was obtained for oligo(A₅-AATAT), which contains an A₅-tract spaced approximately one helical repeat from the AATAT sequence (Table I). Oligomers of oligo(A₅-AATAT) were shown to have a higher electrophoretic retardation than oligomers of oligo(AATAT) (6). In this case, the pattern of \cdot OH reactivity of the AATAT-sequence is also sinusoidal (Figure 1A). Cleavage of the A₅-tract is also sinusoidal. Oligo(ATAAT), which is also found to be intrinsically curved by gel electrophoresis shows a similar, though less pronounced, sinusoidal pattern of \cdot OH cleavage (Figure 1C, upper part). In this case, the maximum of reactivity also occurs either three or four bases upstream from the AT-rich element while the minimum is located at the 5' adenine residue of the AA dinucleotide. When the reaction is performed at 20°C, the pattern of \cdot OH cleavage of oligo(ATAAT) becomes fairly uniform (Figure 1C, lower part). As discussed above, oligo(ATAAT) does not show any significant degree of curvature at this temperature. Similarly, oligo(TAATA), oligo(TATAA) and oligo(ATATA), which are not intrinsically curved as judged by gel electrophoresis, show uniform patterns of \cdot OH cleavage even at 4°C (Figure 1D–F).

The AATAT sequence shows a decreased sensitivity to cleavage by DNase I

A decrease in \cdot OH cleavage has been generally interpreted as indicative of a local narrowing of the minor groove. Therefore, the results reported in Figure 1 suggest that the AT-rich region of the intrinsically curved oligonucleotides has a narrow minor groove. The patterns of DNase I cleavage shown in Figure 2 are in agreement with this interpretation. Cleavage by the nuclease DNase I is sensitive to changes in minor groove width (22–24). Resistance to DNase I cleavage at AT-rich sequences is generally interpreted as reflecting the presence of a narrow minor groove. The pattern of DNase I cleavage of oligo(A₅-AATAT) shows two regions of low frequency of cleavage (Figure 2A). A first region of protection is centred around the A₅-tract, extending from the second adenine of the tract to the cytosine immediately downstream from it (Figure 2D). The DNA region around the AATAT-element is also resistant to DNase I cleavage. Protection

in this case involves the two guanine residues upstream from the tract and extends up to the first thymine residue of the AATAT-element (Figure 2D). These two regions of low frequency of DNase I cleavage correspond to the same regions also showing a decreasing frequency of \cdot OH reactivity (Figure 1A).

Oligo(AATAT), which solely contains the AATAT-element, shows a similar though not identical pattern of DNase I cleavage. Also in this case, the 5' region of the AATAT sequence is resistant to cleavage by DNase I (Figure 2B). However, the GpG step upstream from the AATAT-element is cleaved more efficiently in oligo(AATAT) than in oligo(A₅-AATAT). As a consequence, the region of low frequency of cleavage is one

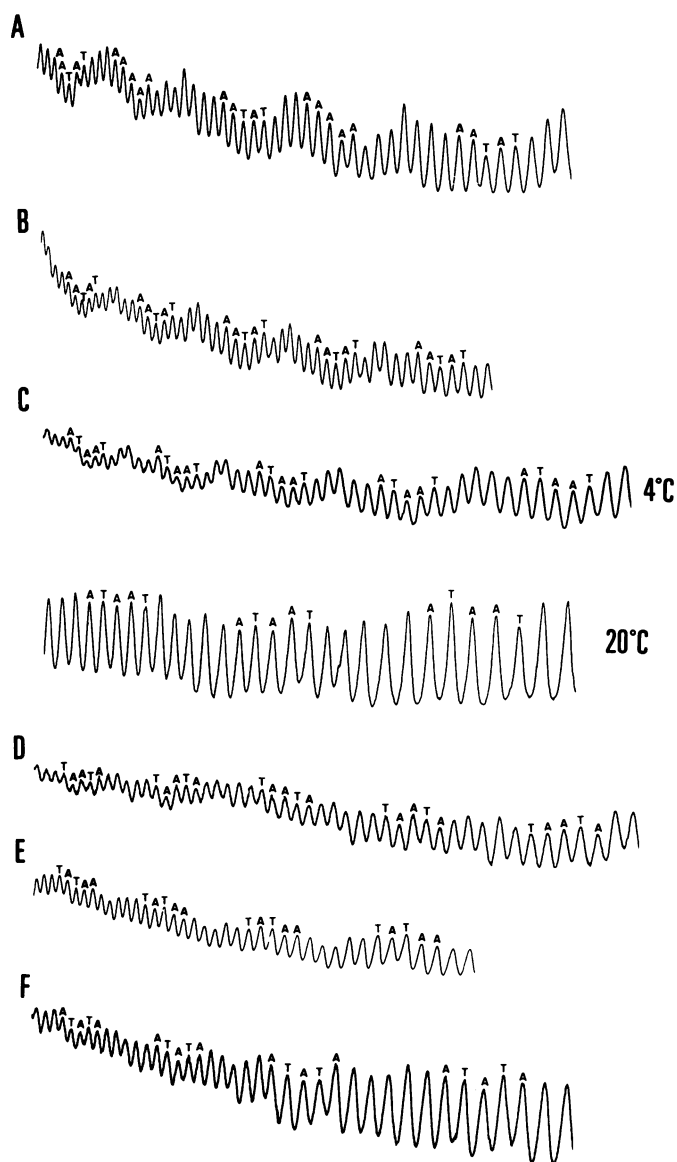


Figure 1. Patterns of hydroxyl radical cleavage of oligo(A₅-AATAT) (A), oligo(AATAT) (B), oligo(ATAAT) (C), oligo(TAATA) (D), oligo(TATAA) (E) and oligo(ATATA) (F). Cleavage by the hydroxyl radical was always performed at 4°C, except in the case of oligo(ATAAT), where the reaction was also carried out at 20°C (C, lower part). Shown are the densitometer scans corresponding to the gel electrophoretic analysis of the cleavage products of each oligonucleotide. The position corresponding to the AT-rich sequences is indicated in each case. The 5'-to-3' direction is left-to-right. Similar results were obtained when the complementary strands were studied.

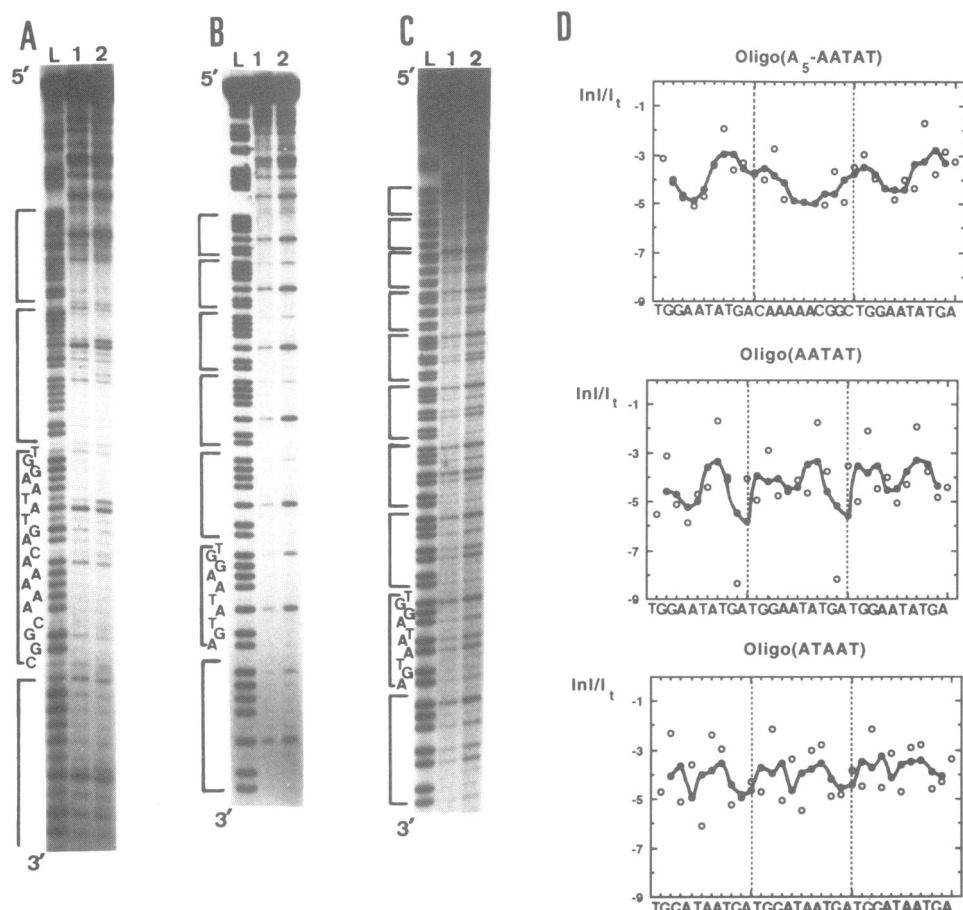


Figure 2. Patterns of DNase I cleavage of oligo(A₅-AATAT) (A), oligo(AATAT) (B) and oligo(ATAAT) (C). DNase I digestion was performed at 5×10^{-3} enzyme units/ μ l (lanes 1) and 2.5×10^{-2} enzyme units/ μ l (lanes 2). Lanes L correspond to the G+A sequencing ladders of each oligonucleotide and the sequence corresponding to the repeating unit is indicated in each case. The position of adjacent repeats is indicated by the brackets. The 5'-to-3' direction is indicated. Quantitative analysis of the results are shown in (D). The actual relative frequency of cleavage (\circ) as well as the three-bond running average of cleavage (\bullet — \bullet) are shown through three consecutive repeats for each oligonucleotide. Similar results were obtained when the complementary strands were studied.

nucleotide shorter (Figure 2D). Again, the same region shows a decreasing frequency of \cdot OH reactivity (Figure 1B). A second difference between the patterns of DNase I cleavage of oligo(AATAT) and oligo(A₅-AATAT) is found at the region downstream from the AATAT-element. This region is significantly less sensitive to DNase I in oligo(AATAT) than in oligo(A₅-AATAT) (compare Figures 2A and 2B). As a consequence, in the case of oligo(AATAT), a second region of low frequency of cleavage is found downstream from the AATAT sequence. As discussed later, this downstream region of low DNase I cutting is likely to arise from the sequence preferences of DNase I cleavage (25).

The AA dinucleotide of the AATAT sequence shows a peculiar reactivity with DEPC

The low \cdot OH and DNase I cleavage rates shown by the AATAT-sequence indicate that this sequence has an altered structural conformation. Additional evidence in favour of this hypothesis comes from the DEPC modification experiments described in Figure 3. DEPC reacts with adenine residues at their N7-group. In general, regular right-handed B-DNA is not reactive to DEPC. However, a strong DEPC reactivity of the 5' adenine residue

of the AA dinucleotide of the AATAT sequence is observed both in oligo(AATAT) and in oligo(A₅-AATAT), the 3' adenine residue being totally unreactive (Figures 3A and 3B). The A₅-tract of oligo(A₅-AATAT) is also reactive with DEPC. Also in this case, the further most 3' adenine residue of the tract is not reactive with DEPC while the remaining four residues of the tract show a strong DEPC reactivity (Figure 3A). This pattern of reactivity is not observed in random sequence DNA (33).

Several intrinsically curved sequences share similar patterns of DNase I and DEPC reactivity

As shown before, the patterns of \cdot OH, DNase I and DEPC reactivity of the intrinsically curved AATAT sequence shows specific features which are similar to those corresponding to an A₅-tract. The question then arises as to what extent these common features are characteristic of intrinsically curved DNA. To address this question the patterns of DNase I and DEPC reactivity of several straight and intrinsically curved oligonucleotides were determined. Oligo(ATAAT) which, as judged by its retarded electrophoretic migration in polyacrylamide gels (Table I), is also intrinsically curved shows a pattern of DNase I cleavage which is very similar to that corresponding

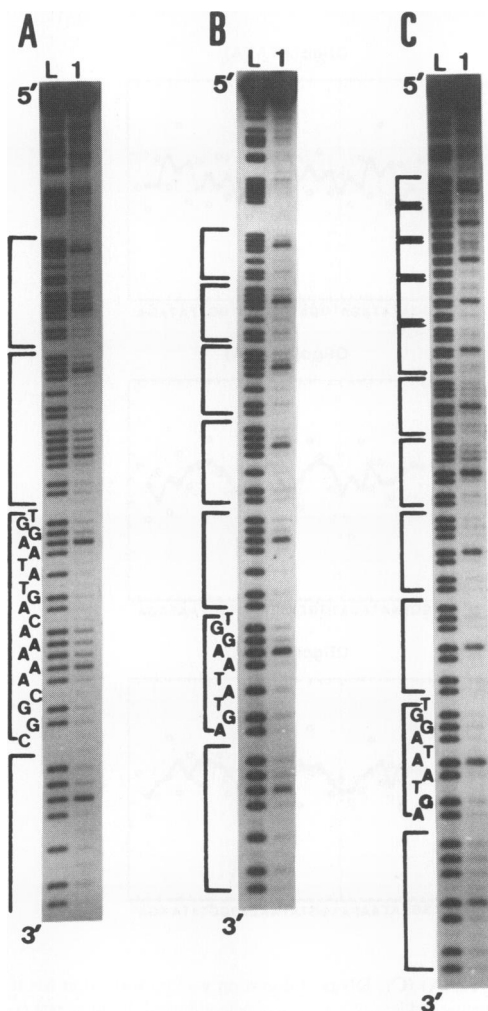


Figure 3. Patterns of DEPC modification of oligo(A₅-AATAT) (A), oligo(AATAT) (B) and oligo(ATAAT) (C). Lanes 1 correspond to the DEPC modification products of each oligonucleotide. Lanes L correspond to the G+A sequencing ladders of each oligonucleotide and the sequence corresponding to the repeating unit is indicated in each case. The position of adjacent repeats is indicated by the brackets. The 5'-to-3' direction is indicated.

to oligo(AATAT) (Figure 2C). A region of low frequency of cleavage is detected 5' from the AT-rich sequence (Figure 2D). However, protection in this case is significantly less pronounced than in the cases of oligo(AATAT) and oligo(A₅-AATAT). The region downstream from the AT-region is, also in this case, resistant to DNase I cleavage. In oligo(ATAAT), the AA dinucleotide shows the peculiar DEPC reactivity described before; the 5' adenine residue is reactive with DEPC while the 3' residue is not (Figure 3C).

On the other hand, oligo(TATAA) and oligo(ATATA), which are not intrinsically curved, show patterns of DNase I cleavage which are significantly different from those corresponding to the oligonucleotides which are curved. In the case of oligo(ATATA), steps showing a relatively high frequency of cleavage alternate with steps showing low frequency of cleavage (Figure 4A), and no real protection from DNase I digestion is detected in any region of the oligonucleotide (Figure 4D). In the case of oligo(TATAA), the 5' region of the AT-rich sequence is

significantly cleaved by the nuclease (Figure 4C), and no resistance to DNase I cleavage is observed at this region (Figure 4D). However, in this case, the region of low frequency of cleavage located downstream from the AT-sequence is still observed (Figure 4D). In addition, no strong DEPC reactivity of the adenine residues is observed in either oligo(ATATA) or oligo(TATAA) (Figures 5A and 5C). In the case of oligo(TATAA), the 5' adenine residue of the AA dinucleotide still reacts with DEPC though to a much lesser extent than in any of the intrinsically curved oligonucleotides described before.

Oligo(TAATA) constitutes an exception to this behaviour since, despite not being intrinsically curved, shows DNase I and DEPC reactivity patterns similar to those corresponding to the intrinsically curved oligonucleotides. A region of low frequency of DNase I cleavage is detected at the 5' region of the TAATA sequence (Figure 4B). This protection from DNase I digestion is weaker than that observed in the case of oligo(AATAT) but is not significantly different from that detected in the case of oligo(ATAAT) (Figure 2). Furthermore, the AA dinucleotide of oligo(TAATA) shows the same pattern of DEPC reactivity described before for oligo(AATAT) (Figure 5B). It is known that the curvature induced by an A-tract is influenced by the nature of the adjacent sequences (9). It is interesting to note that both oligo(TAATA) and oligo(TATAA), which are not intrinsically curved, contain precisely the same dinucleotide steps immediately adjacent to the AT-sequence. In both cases, a GpT step is found 5' from the AT-sequence and an ApG step is located 3' of it. This suggests that the presence of particular flanking steps might have an influence or even abolish the curvature induced by an AT-rich sequence. To investigate this question the electrophoretic behaviour of oligomers of oligo(AATATA), which contains a 3½ ApG step, and of oligo(TAATAT), which contain a 5½ GpT step, was analyzed. In both cases, a significant retardation was observed (Table I), indicating that both oligonucleotides are intrinsically curved. Moreover, the patterns of DNase I and DEPC reactivity of oligo(AATATA) and oligo(TAATAT) are very similar to those obtained in the case of oligo(AATAT). The 5' region, but not the 3' region, of oligo(AATATA) and oligo(TAATAT) are resistant to cleavage by DNase I (Figure 6C) and, in both cases, the AA dinucleotide shows the peculiar reactivity with DEPC described above (Figures 6A and 6B, lanes 3). These results show that the lack of curvature of oligo(TATAA) and oligo(TAATA) cannot be accounted by the chemical nature of the flanking steps. However, a detailed comparison of the patterns of DNase I cleavage of the straight and intrinsically curved oligonucleotides shown in Figures 2, 4 and 6, reveals some important differences in the frequency of cleavage of the steps flanking the AT-region (Figure 7). In the cases of the intrinsically curved oligonucleotides, the flanking steps are always cleaved poorly (Figure 7A–C and G). On the other hand, in the case of oligo(TAATA), which is not curved, both the 5' GpT and the 3' ApG flanking steps are strongly cleaved (Figure 7E). The high frequency of cleavage of the 5' GpT step is not constrained to the case of oligo(TAATA). The same 5' GpT step is present in oligo(TATAA), which is not curved either, and in oligo(TAATAT), which is curved, and in both cases the step is strongly cleaved (Figure 7F and H). However, strong cleavage at the 3' ApG step appears to be specific of oligo(TAATA). The same 3' ApG step also occurs in oligo(TATAA) and oligo(ATATA), which are not curved, and in oligo(AATATA), which is curved, and, in all these cases, it shows a rather low frequency of cleavage (Figure 7D, F and G).

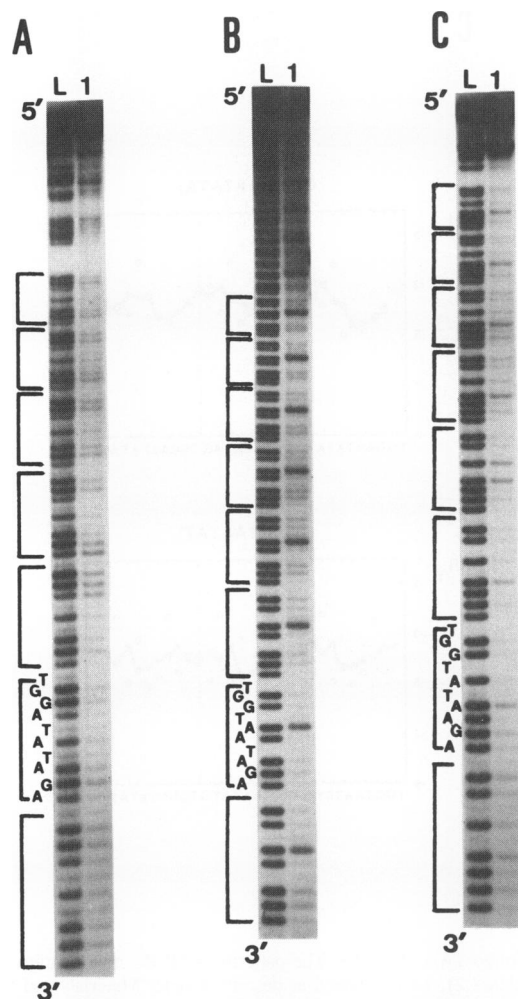


Figure 5. Patterns of DEPC modification of oligo(ATATA) (A), oligo(TAATA) (B) and oligo(TATAA) (C). Lanes L correspond to the DEPC modification products of each oligonucleotide. Lanes L correspond to the G+A sequencing ladders of each oligonucleotide and the sequence corresponding to the repeating unit is indicated in each case. The position of adjacent repeats is indicated by the brackets. The 5'-to-3' direction is indicated.

must, also in this case, be the result of the vectorial addition of the deflection of the helical axis occurring at each dinucleotide step. However, the magnitude and/or direction of the deflection occurring at each step must depend on the precise nucleotide sequence. The patterns of $\cdot\text{OH}$, DNase I and DEPC reactivity of oligo(A₅-AATAT) and oligo(AATAT) indicate that the AATAT sequence has an altered structure. This altered conformation is characterized by: (1) the presence of a narrow minor groove, as indicated by the decrease in the frequencies of cleavage by DNase I and $\cdot\text{OH}$ and (2) a distorted conformation of the ApA step, as reflected by the hyperreactivity to DEPC of the 5' adenine residue.

Abundant biochemical and crystallographic data indicate that cleavage by DNase I is mainly influenced by the global structural characteristics of the grooves (22–25, 41, 42). DNase I cleavage is also influenced by the local conformational parameters of each phosphodiester bond (29–32, 43). As a consequence, the frequency of cleavage at each individual dinucleotide step changes significantly from one step to the next. However, the fluctuation

of the cleavage rate along any DNA fragment can be eliminated to a large extent by averaging the frequency of cleavage of each individual step with those of its nearest neighbours. This three-bond running average of cleavage reflects better the geometry of the minor groove and it has been widely used to monitor changes in minor groove width (8, 22–24). In this way, a region of low frequency of cleavage was detected at the 5' region of the AATAT sequence suggesting the presence of a narrow minor groove in this region. In good agreement with this interpretation, the same region shows a decreased sensitivity to cleavage by the $\cdot\text{OH}$. Though, the structural basis of the cleavage by the $\cdot\text{OH}$ is not completely understood, all the available experimental evidence strongly suggest that it is sensitive to the geometry of the minor groove. The decrease in the cutting frequency is consistent with the narrowing of the minor groove, which is likely to reduce the accessibility of the sugar residues being attacked by the $\cdot\text{OH}$ (18).

In the case of oligo(AATAT), an additional region of low DNase I cleavage is found downstream from the AATAT sequence. The frequency of cleavage of this region is principally determined by the very low rate of cleavage of the GpA step located 3' from the AATAT sequence. This GpA step is much less sensitive to DNase I in oligo(AATAT) than in oligo(A₅-AATAT) (Figures 7A and B). It is known that DNase I cleavage shows some sequence preferences (25). Actually, in the case of oligo(AATAT), the GpA step is found within the context of the hexanucleotide ATGATG which is known to render this step fairly resistant to the nuclease (25). The same hexanucleotide is found in oligo(ATAAT) and, also in this case, the GpA step is cleaved poorly (Figure 7C). Finally, this downstream region of low frequency of DNase I cleavage is not observed in oligonucleotides that, as oligo(AATATA) and oligo(TAATAT), do not contain a GpA step downstream from the AT-region. Therefore, this additional region of low cutting is likely to reflect the sequence preferences of DNase I cleavage rather than the presence of a narrow minor groove. Consistent with this interpretation, the frequency of $\cdot\text{OH}$ cleavage does not decrease along this region.

The AA dinucleotide of the AATAT sequence shows a characteristic reactivity with DEPC. The 5' adenine residue is hyperreactive to DEPC while the 3' residue is completely unreactive. Others have reported similar patterns of DEPC modification for different A-tracts (26–28). This peculiar DEPC reactivity corroborates the hypothesis that the AATAT sequence has an altered structural conformation. However, the lack of knowledge about the chemical basis of the reactivity of adenine residues with DEPC, makes it difficult to unambiguously determine the structural conformation which is responsible for this DEPC hyperreactivity. Structural models in which, through an increase in tilt, roll or propeller twist, the adenine N7-groups become more accessible to the solvent are compatible with these results.

All of the intrinsically curved oligonucleotides described here show patterns of $\cdot\text{OH}$, DNase I and DEPC reactivity which are similar to those obtained in the case of the AATAT sequence. On the other hand, the patterns of reactivity obtained in the cases of oligo(TATAA) and oligo(ATATA), which are not intrinsically curved, show different features. These results strongly suggest that all the intrinsically curved oligonucleotides described in this paper share a common structural conformation which is different from that corresponding to the oligonucleotides showing no

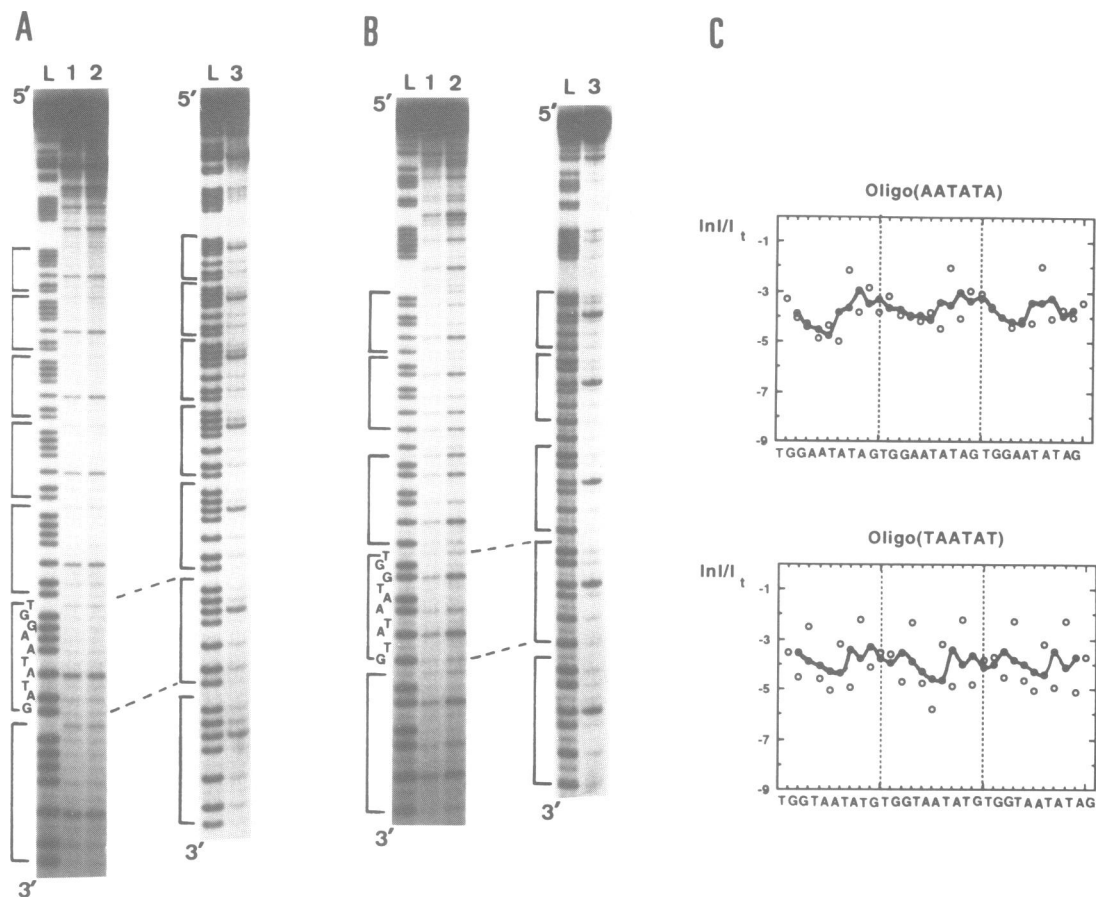


Figure 6. Patterns of DNase I cleavage and DEPC modification of oligo(AATATA) (A) and oligo(TAATAT) (B). The patterns of DEPC modification (lanes 3) and DNase I cleavage at 5×10^{-3} enzyme units/ μ l (lanes 1) and 2.5×10^{-2} enzyme units/ μ l (lanes 2), were obtained as described under Materials and Methods. Lanes L correspond to the G+A sequencing ladders of each oligonucleotide and the sequence corresponding to the repeating unit is indicated in each case. The position of adjacent repeats is indicated by the brackets. The 5'-to-3' direction is indicated. Quantitative analysis of the DNA I cleavage patterns are shown in (C). The actual relative frequency of cleavage (\circ) as well as the three-bond running average of cleavage (\bullet - \bullet) are shown through three consecutive repeats for each oligonucleotide. Similar results were obtained when the complementary strands were studied.

significant curvature. As discussed before, oligo(TAATA) constitutes an exception to this general behaviour. This oligonucleotide, despite of not showing a significant retardation in polyacrylamide gels, shows a region of low frequency of DNase I cleavage located 5' from the AT-sequence and the characteristic hyperreactivity to DEPC of the ApA step. The reason for this discrepancy is not totally clear. DNase I cleavage is performed in the presence of Mg and it has been recently reported that the electrophoretic retardation of some intrinsically curved oligonucleotides is increased in the presence of some divalent cations, in particular of Mg (44). This effect is very strong for GC-rich oligonucleotides and only moderate for oligonucleotides containing phased A-tracts. Therefore, it might be possible that oligo(TAATA) would be curved under the DNase I digestion conditions, providing a reasonable explanation for its decreased sensitivity to cleavage by the nuclease. However, the pattern of DEPC reactivity of oligo(TAATA), which was obtained in the absence of any added metal ion, strongly suggest that the TAATA sequence also adopts an altered structure in the absence of divalent cations, under conditions which are close to the gel electrophoretic conditions. An alternative explanation to this behaviour comes from the DNase I cleavage data reported

in Figure 7. In the case of oligo(TAATA), the 3' flanking ApG step shows an anomalously high rate of cleavage. The same 3' ApG step also occurs in oligo(TATAA), oligo(ATATA) and oligo(AATATA) and, in all these cases, it shows a rather low frequency of cleavage (Figure 7D, F and G). It is important to notice that the 3' ApG step of oligo(ATATA) is contained within exactly the same ATAGATGG-sequence context as in oligo(TAATA). Therefore, it is unlikely that the high frequency of cleavage of this step in oligo(TAATA) would be the consequence of the sequence preferences of DNase I cleavage. It might, in this case, reflect a particular conformational feature associated with the step. It was proposed that the rate of cleavage of any individual phosphodiester bond by DNase I is highly influenced by the twist angle associated with it (29,30). Therefore, it is possible that the high cleavage rate of the 3' ApG step of oligo(TAATA) would reflect, in this case, a particularly high twist of the step. It has been proposed that curvature induced by an A-tract occurs principally at the junctions between the A-tract and the surrounding B-type DNA. In this model, deflection of the helical axis occurs principally at the 3' junction (9); the 5' junction contributing to a much lesser extent. Therefore, it is feasible that the precise conformational parameters associated

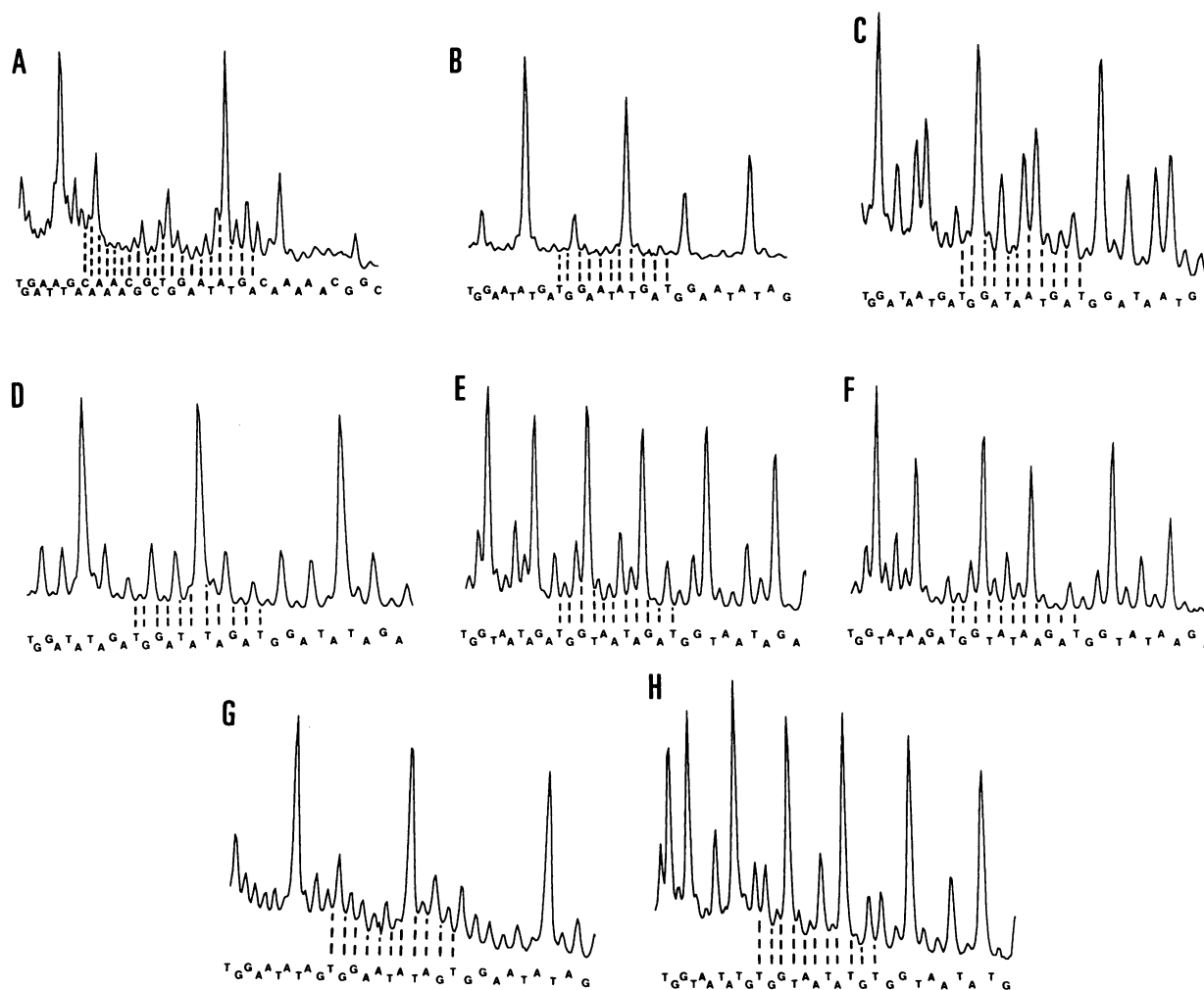


Figure 7. Profiles of DNase I cleavage of oligo(A₅-AATAT) (A), oligo(AATAT) (B), oligo(ATAAT) (C), oligo(ATATA) (D), oligo(TAATA) (E), oligo(TATAA) (F), oligo(AATATA) (G) and oligo(TAATAT) (H). The densitometer scans corresponding to lanes 2 of Figures 2, 4 and 6 are shown through three consecutive repeats for each oligonucleotide. The 5'-to-3' direction is always left-to-right. Each peak on the densitometer scan corresponds to cleavage of the P-O3' bond of the nucleotide 5'.

with the 3' flanking step would have a strong influence on the degree of curvature. An increased twist at the 3' junction might reduce the magnitude of the global bending by changing the direction of the 3' bend with respect to the 5' bend.

In summary, our results indicate that curvature induced by the AATAT element is the direct consequence of its altered structural properties. Abundant crystallographic evidence also indicates that A-tracts do not adopt a canonical B-DNA conformation (34–37). In all these crystal structures, A-tracts show a narrow minor groove and a large propeller twist. In all these cases, the A-tracts are rather straight suggesting that deflection of the helical axis is taking place outside of the A-tract. Based also on crystallographic evidence (38), it was recently proposed that A-tracts do not induce any bending by themselves and that the intrinsic curvature of A-tract containing DNA molecules is the consequence of the conformational properties of the DNA sequences located in between phased A-tracts. In particular, the GGC sequence, which is found in most intrinsically curved DNA molecules studied so far, was shown to exhibit a major-groove-

compressing bend. This is not likely to be the explanation for the effects described here since, among all the intrinsically curved oligonucleotides studied in this paper, only oligo(A₅-AATAT) contains this GGC sequence (Table I). Furthermore, oligo(TAATA), oligo(TATAA) and oligo(ATATA), which are not curved, contain exactly the same spacing sequence than oligo(AATAT) and oligo(ATAAT), which are curved.

ACKNOWLEDGEMENTS

We are thankful to N.Ferrer and M.Ortiz-Lombardía, for experimental help, and to Dr M.Coll and Dr J.Portugal, for carefully reading this manuscript. This work was financed by grants from the DGICYT (PB90-997 and CE93-0002), the CEC (BIOT-CT91-256) and the Generalitat de Catalunya. PC acknowledges receipt of a doctoral fellowship from the Ministerio de Educacin y Ciencia.

REFERENCES

1. Trifonov, E. N. (1985) *CRC Crit. Rev. Biochem.* **19**, 89–106.
2. Hagerman, P. J. (1990) *Annu. Rev. Biochem.* **59**, 755–781.
3. Hagerman, P. J. (1992) *Biochim. Biophys. Acta* **1131**, 125–132.
4. Bolshoy, A., McNamara, P., Harrington, R.E., and Trifonov, E.N. (1991) *Proc. Natl. Acad. Sci. USA* **88**, 2312–2316.
5. McNamara, P. T., and Harrington, R. E. (1991) *J. Biol. Chem.* **266**, 12548–12554.
6. Carrera, P., Martínez-Balbás, M. A., Portugal, J., and Azorín, F. (1991) *Nucleic Acids Res.* **19**, 5639–5644.
7. Bruckner, I., Jurukovski, V., Konstantinovic, M., and Savic, A. (1991) *Nucleic Acids Res.* **19**, 3549–3551.
8. Bruckner, I., Dlakic, M., Savic, A., Susic, S., Pongor, S., and Suck, D. (1993) *Nucleic Acids Res.* **21**, 1025–1029.
9. Koo, H.-S., Wu, H.-M., and Crothers, D.M. (1986) *Nature* **320**, 501–506.
10. Chuprina, V.P. (1987) *Nucleic Acids Res.* **15**, 293–311
11. Koo, H.-S., and Crothers, D. M. (1988) *Proc. Natl. Acad. Sci. USA* **85**, 1763–1767.
12. Nadeau, J.G., and Crothers, D.M. (1989) *Proc. Natl. Acad. Sci. USA* **86**, 2622–2626.
13. Ulanovsky, L. E., Bodner, M., Trifonov, E. N., and Choder, M. (1986) *Proc. Natl. Acad. Sci. USA* **83**, 862–866.
14. Ulanovsky, L. E., and Trifonov, E. N. (1987) *Nature* **326**, 720–722.
15. Calladine, C. R., Drew, H.R., and McCall, M. J. (1988) *J. Mol. Biol.* **201**, 127–137.
16. Zurkhin, V. B., Ulyanov, N. B., Gorin, A. A., and Jernigan, R. L. (1991) *Proc. Natl. Acad. Sci. USA* **88**, 7046–7050.
17. Sanger, F., Nicklen, S., and Coulson, A. R. (1977) *Proc. Natl. Acad. Sci. USA* **74**, 5463–5476.
18. Burkhoff, A. M., and Tullius, T. D. (1987) *Cell* **48**, 935–943.
19. Burkhoff, A. M., and Tullius, T. D. (1988) *Nature* **331**, 445–457.
20. Price, M. A., and Tullius, T. D. (1993) *Biochemistry* **32**, 127–136.
21. Tullius, T. D., and Dombrosky, B. A. (1985) *Science* **230**, 679–681.
22. Drew, H. R. (1984) *J. Mol. Biol.* **176**, 535–557.
23. Drew, H. R., and Travers, A. A. (1984) *Cell* **37**, 491–502.
24. Lahm, A., and Suck, D. (1991) *J. Mol. Biol.* **221**, 645–667.
25. Herrera, J. E., and Chaires, J. B. (1994) *J. Mol. Biol.* **236**, 405–411.
26. McCarthy, J. G., Williams, L. D., and Rich, A. (1990) *Biochemistry* **29**, 6071–6081.
27. McCarthy, J. G., and Rich, A. (1991) *Nucleic Acids Res.* **19**, 3421–3429.
28. McCarthy, J. G., Frederick, C. A., and Nicolas, A. (1993) *Nucleic Acids Res.* **14**, 3309–3317.
29. Lomonosoff, G. P., Butler, P. J. G., and Klug, A. (1981) *J. Mol. Biol.* **149**, 745–760.
30. Dickerson, R. E., and Drew, H. R. (1981) *J. Mol. Biol.* **149**, 761–786.
31. Hogan, M. E., Roberson, M. W., and Austin, R. H. (1989) *Proc. Natl. Acad. Sci. USA* **86**, 9273–9277.
32. Bruckner, I., Jurukovski, V., and Savic, A. (1990) *Nucleic Acids Res.* **18**, 891–894.
33. Portugal, J., Fox, K.R., McLean, M.J., Richenberg, J.L., and Waring, M.J. (1988) *Nucleic Acids Res.* **16**, 3655–3670.
34. Wing, R.M., Drew, H.R., Takano, T., Broke, C., Tanaka, S., Itakura, K., and Dickerson, R.E. (1980) *Nature* **287**, 755–758.
35. Nelson, H.C.M., Finch, J.T., Luisi, B.F., and Klug, A. (1987) *Nature* **330**, 221–226.
36. Coll, M., Frederick, C.A., Wang, A.H.-J., and Rich A. (1987) *Proc Natl. Acad. Sci. USA* **86**, 8385–8389.
37. DiGabriele, A.D., Sanderson, M.R., and Steitz, T.A. (1989) *Proc. Natl. Acad. Sci. USA* **86**, 1816–1820.
38. Goodsell, D.S., Kopka, M.L., Cascio, D., and Dickerson, R.E. (1993) *Proc. Natl. Acad. Sci. USA* **90**, 2930–2934.
39. Mujeeb, A., Kerwin, S.M., Kenyon, G.L., and James, T.L. (1993) *Biochemistry* **32**, 13419–13431.
40. Weisz, K., Shafer, R.H., Egan, W., and James, T.L. (1994) *Biochemistry* **33**, 354–366.
41. Suck, D., Lahm, A., and Oefner, C. (1988) *Nature* **332**, 462–468.
42. Weston, S.A., Lahm, A., and Suck, D. (1992) *J. Mol. Biol.* **226**, 1237–1256.
43. Fox, K.R. (1992) *Nucleic Acids Res.* **20**, 6487–6493.
44. Bruckner, I., Susic, S., Dlakic, M., Savic, A., and Pongor, S. (1994) *J. Mol. Biol.* **236**, 26–28.